Energy, Mines and Resources Canada

Énergie, Mines et Ressources Canada

CANMET

Canada Centre for Mineral and Energy Technology

Centre canadien de la technologie des minéraux et de l'énergie

Mining Research Laboratories

Laboratoires de recherche minière

Canada

MRL 88-39 (TR) c. 2

1-7987298 c.2
CPUB

ANISOTROPIC PROPERTIES STUDY OF LAC DU BONNET GRANITE SPECIMENS: REPORT #5

R. Jackson

MRL 88-39 (TR)

May 1988

1-7987298 c.2
CPUB

ANISOTROPIC PROPERTIES STUDY OF LAC DU BONNET GRANITE SPECIMENS: REPORT #5

by

Rand Jackson*

ABSTRACT

Compressive and shear wave velocity measurements, as well as uniaxial compression testing, were conducted on samples obtained from boreholes located in the Lac du Bonnet batholith near Pinawa, Manitoba. The purpose of the study is to ascertain if any anisotropy in terms of the uniaxial mechanical properties exists in the Lac du Bonnet samples and, if so, to what extent.

This is the fifth in a series of anisotropy reports and offers a summary of all data generated to date. Also included are the best fit ellipsoids calculated for the uniaxial compressive strengths, 50% secant and 50% tangent moduli of each borehole.

Mean maximum anisotropies for all boreholes of 1.54, 1.33 and 1.31 were determined for the uniaxial compressive strength, 50% secant and 50% tangent moduli, respectively. Statistical analysis of the 50% tangent moduli values, however, indicated that results from boreholes 001-041-MOD1, 206-012-MOD1 and 001-275-MOD2 did not belong to the same population as the remaining nine holes. Eliminating these holes results in a mean maximum 50% tangent modulus anisotropy of 1.13 which indicates a relatively isotropic rock type in terms of deformational properties at stress levels equal to 50% of the uniaxial failure strength.

It is recommended that all results be rotated into a common coordinate axis where one ellipsoidal fit can be conducted. Further analysis of the secant and tangent moduli determined at stress levels comparable to those found on the operating levels of the URL is also recommended.

---

*Research Officer, Canadian Mine Technology Laboratory, CANMET, Energy, Mines and Resources Canada, Ottawa, Ontario.

Keywords

Anisotropy, Rock Properties, Mechanical, Young's Modulus, Poisson's Ratio, Uniaxial Compressive Strength, Velocity, Lac du Bonnet

CANMET LIBRARY
3 2329 00061436 7
c.2
CPUB

ETUDE DES PROPRIETES ANISOTROPES D'ECHANTILLONS DE GRANITE DU LAC DU BONNET: RAPPORT NO. 5

par

Rand Jackson*

RÉSUMÉ

Des mesures des vitesses des ondes de compression et de cisaillement, ainsi que des essais de compression uniaxiale, ont été effectués sur des échantillons recueillis à partir de sondages réalisés dans le batholite du lac du Bonnet, à proximité de Pinawa (Manitoba). L'étude vise à déterminer s'il existe quelque anisotropie quant aux propriétés mecaniques uniaxiales dans les échantillons du lac du Bonnet et, le cas échéant, l'importance de cette anisotropie.

Le présent rapport est le cinquième d'une série de rapports sur l'anisotropie et il contient un résumé de toutes les données produites à ce jour. Il contient aussi les ellipsoïdes les mieux lissées établies en fonction de la résistance à la compression uniaxiale, du module sécant 50% et du module tangent 50% pour chaque sondage.

Des anisotropies maximales moyennes pour tous les sondages de 1,54, 1,33 et 1,31 ont été obtenues pour la résistance à la compression uniaxiale, le module sécant 50% et le module tangent 50% respectivement. Toutefois, l'analyse statistique des valeurs du module tangent 50% a montré que les résultats pour les sondages 001-041-MOD1, 206-012-MOD1 et 001-275-MOD2 n'appartenaient pas à la même population que ceux des neuf autres sonages. L'élimination des résultats obtenus pour ces sondages donne une anisotropie maximale moyenne pour le module tangent 50% de 1,13, ce qui signfie que la roche est d'un type relativement isotrope quant aux propriété de déformation à des niveaux de contrainte correspondant à 50% de la résistance à la rupture uniaxiale.

On recommande de faire subir à tous les résultats une rotation suivant un axe de coordonnées commun auquel on peut appliquer un lissage ellipsoïdal. On recommande aussi d'effectuer un analyse du module sécant et du module tangent déterminés à des niveaux de contrainte comparable à ceux qui ont été obtenus aux niveaux de fonctionnement du LRS.

---

*Chercheur, Laboratoire canadien de technologie minière, Laboratoires de recherche minière, CANMET, Énergie, Mines et Ressources Canada, Ottawa (Ontario).

Mots clés

Anisotropie, propriétés des roches, mécanique, module tangentiel de Young, rapport de Poisson, résistance à la compression uniaxiale, vitesse, lac du Bonnet

CONTENTS

TABLES

FIGURES

INTRODUCTION

As part of the Canadian Nuclear Fuel Waste Management Project, Atomic Energy of Canada Limited is characterizing various rock formations to determine their suitability for long term disposal of high level wastes. The program includes the construction of an underground research laboratory (URL) near Pinawa, Manitoba to provide an opportunity for extensive in situ investigations.

Biaxial testing conducted on core obtained during the construction phase of the URL has indicated that the rock may be anisotropic in terms of modulus of elasticity, (Lang, 1985). It was felt that further study in the form of acoustic velocity and uniaxial compression measurements could provide additional insight into this behaviour.

This report summarizes the results of the program to date and offers some interpretation as to the maximum anisotropies indicated by the data.

IDENTIFICATION OF SPECIMENS AND TESTS

One hundred and twenty-four specimens originating from 14 boreholes have been tested under this program thus far. Borehole identification, location and orientation are summarized as follows;

206-010-MOD1:	Collar coordinates:	N 5,570,460.232
		E 295,789.288
		elev. 52.905
	Orientation:	plunge = 00.60°
		trend (direction) = 025°
206-012-MOD1:	Collar coordinates:	N 5,570,459.711
		E 295,799.653
		elev. 53.186
	Orientation:	plunge = −02.51° (up)
		trend (direction) = 024.16°
206-016-MOD1:	Collar coordinates:	N 5,570,457.186
		E 295,802.432
		elev. 53.255
	Orientation:	plunge = −02.99° (up)
		trend (direction) = 113.95°

206-013-MOD1:	Collar coordinates:	N 5,570,459.138
		E 295,801.045
		elev. 52.674
	Orientation:	plunge = −00.86° (up)
		trend (direction) = 020.97°
001-041-MOD1:	Collar coordinates:	N 5,570,476.120
		E 295,787.639
		elev. 41.089
	Orientation:	plunge = −02.68° (up)
		trend (direction) = 069.09°
001-041-MOD2:	Collar coordinates:	N 5,570,473.642
		E 295,785.900
		elev. 40.637
	Orientation:	plunge = −01.70° (up)
		trend (direction) = 157.78°
001-072-MOD1:	Collar coordinates:	N 5,570,477.032
		E 295,787.329
		elev. 73.518
	Orientation:	plunge = −00.20° (up)
		trend (direction) = 040.98°
001-072-MOD2:	Collar coordinates:	N 5,570,475.026
		E 295,787.969
		elev. 73.308
	Orientation:	plunge = −00.39° (up)
		trend (direction) = 101.04°
001-228-MOD1:	Collar coordinates:	N 5,570,473.089
		E 295,785.897
		elev. 228.546
	Orientation:	plunge = −01.16° (up)
		trend (direction) = 158.72°
001-228-MOD2:	Collar coordinates:	N 5,570,476.277
		E 295,787.783
		elev. 228.327
	Orientation:	plunge = −00.32° (up)
		trend (direction) = 062.09°

001-275-MOD1:	Collar coordinates:	N 5,570,474.047
		E 295,786.956
		elev. 275.626
	Orientation:	plunge = −01.26° (up)
		trend (direction) = 155.12°
001-275-MOD2:	Collar coordinates:	N 5,570,476.094
		E 295,787.377
		elev. 275.634
	Orientation:	plunge = 00.00°
		trend (direction) = 067.38°
101-S09-MOD1:	Collar coordinates:	N 5,570,466.087
		E 295,785.878
		elev. 160.250
	Orientation:	plunge = −03.22° (up)
		trend (direction) = 111.07°
101-S02-MOD1:	Collar coordinates:	N 5,570,475.061
		E 295,789.119
		elev. 160.580
	Orientation:	plunge = −02.89° (up)
		trend (direction) = 026.80°

Two hundred millimeter diameter cores were initially obtained from areas of specific interest at the URL site. These were recored such that three 45mm diameter samples corresponded to orthogonal axes within the larger core. Six additional samples were also recored to correspond to the trisectors of each group of two axes (see Figure 1).

The specimens were then identified according to their location and orientation as follows;

A: depth of the collar of the 45 mm hole from the collar of the 200 mm hole

B: angle β gives the location of the collar of the 45 mm hole around the circumference of the 200 mm core. The angle is measured clock-wise (looking down hole) from the orientation mark on the top of the core.

C: angle α is the angle between the core axis of the 45 mm core and the 200 mm core. The angle is measured clockwise (i.e. dip) from the down hole direction of the 200 mm core.

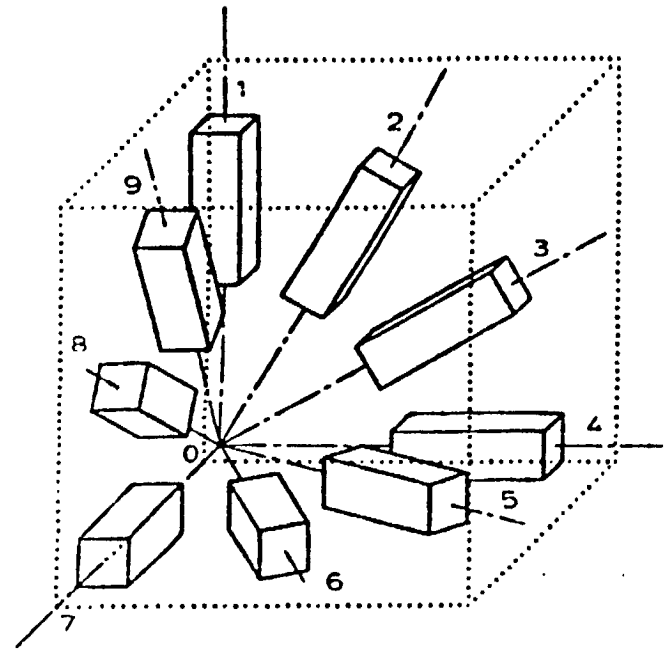

Figure 1: Core Orientations for Anisotropy Specimens (after Peres-Rodrigues, 1967)

Table 1 provides a summary of the specimen depth, dimensions, density and orientation. The following properties were determined for the samples listed;

1) compressive wave velocity
2) shear wave velocity
3) dynamic shear modulus
4) dynamic Young's modulus
5) Poisson's ratio (determined using velocity data)
6) uniaxial compressive strength
7) Poisson's ratio
8) 50% tangent modulus of elasticity
9) 50% secant modulus of elasticity

DESCRIPTION OF TEST MEASUREMENTS

Compressive and shear wave velocity measurements were carried out on samples prior to being gauged for elastic deformation measurement. The testing equipment consisted of: transmitting and receiving platens containing piezoelectric transducers, a high voltage pulse generator, a signal amplifier and a Tektronix Type 555 dual beam oscilloscope equipped with delay sweep and a time base resolution of 0.01 micro-seconds. The zero time delay was determined by measuring the time of wave arrival across three steel samples of different lengths. These arrival times could then be extrapolated to correspond to a specimen of zero length.

For an outline of the uniaxial compression procedure, the reader is referred to Technical Data 303410-M01/78 (Annor and Geller, 1978). The two Phillips PR 9302

strain bridges and the Mosely Autograph 2FRA X-Y recorder referred to in that document were replaced, in the present study, by two Bruel and Kjaer Type 1526 strain indicators and a Hewlett Packard 7046B X-Y recorder. These equipment were used to measure and record the axial and transverse strains as a function of axial load. Linear variable differential transducers (LVDT's) were also utilized to provide redundant measurements of axial deformation.

DATA TREATMENT

The compressive and shear wave velocities were determined by dividing the specimen length by the wave travel time through the specimen. The dynamic properties were then calculated using the following equations (4);

Dynamic Young's Modulus†

$$E_d = \frac{\rho V_s^2 (3V_p^2 - 4V_s^2)}{V_p^2 - V_s^2} \tag{1}$$

where; E_d =dynamic Young's modulus
V_s =shear wave velocity
V_p =compressive wave velocity
ρ =density

Dynamic Young's Modulus*

$$E_d = \frac{V_p^2 \rho (1+\nu)(1-\nu)}{(1-\nu)} \tag{2}$$

where; E_d =dynamic Young's modulus
V_p =compressive wave velocity
ρ =density
ν =Poisson's ratio=.25

Dynamic Shear Modulus

$$G_d = \rho V_s^2 \tag{3}$$

where; G_d =dynamic shear modulus
V_s =shear wave velocity
ρ =density

† Used when shear wave velocity measurements were available.
* Used when shear wave velocity measurements were not available.

Poisson's Ratio (based on velocity data)

$$\nu_d = \frac{V_p^2 - 2V_s^2}{2(V_p^2 - V_s^2)} \tag{4}$$

where; ν_d =Poisson's ratio
V_s =shear wave velocity
V_p =compressive wave velocity

Due to equipment failure, both compressive and shear wave velocity data are unavailable for boreholes 206-016-MOD1 and 001-041-MOD1 while only compressive wave data is available for borehole 101-S09-MOD1. An estimated Poisson's ratio of 0.25 was used to calculate the dynamic shear moduli for hole no. 101-S09-MOD1. The tangent modulus of elasticity (E_t) was calculated for each sample by determining the slope of the tangent to the axial strain curve at 50% of the failure load. The 50% secant modulus of elasticity (E_s)was calculated by determining the slope of the line joining the origin to the point on the axial strain curve corresponding to 50% of the failure load. The ultimate compressive strength (σ_c) of each sample was calculated by dividing the sample failure load by the sample's cross-sectional area. The ratio of the tangent to the axial strain curve to the tangent to the transverse strain curve at 50% failure load was used to determine the sample's Poisson's ratio (ν). The reader is asked to refer to MRL Division Reports M&ET/MRL 86-48(TR), 86-79(TR), 86-142(TR) and 87-104(TR) for the uniaxial stress-strain curves.

As stated earlier, the samples were cored from a 200mm diameter borehole to correspond to three orthogonal axes and their trisectors. It is then possible to resolve the mechanical properties of interest into x, y and z coordinates according to a cartesian system defined by those orthogonal axes. The points thus derived are then fitted to an ellipsoid-type quadratic equation defined as;

$$\begin{pmatrix} x & y & z \end{pmatrix} \begin{pmatrix} \alpha_1 & \alpha_2 & \alpha_3 \\ \alpha_2 & \alpha_4 & \alpha_5 \\ \alpha_3 & \alpha_5 & \alpha_6 \end{pmatrix} \begin{pmatrix} x \\ y \\ z \end{pmatrix} = 10^5 \tag{5}$$

The most probable values of the α_i coefficients were calculated using the method of least squares from the nine results determined for the recored specimens.

The standard form of each ellipsoid was subsequently obtained using a suitable rotation of the coordinate axes. The maximum degree of anisotropy could then be calculated by determining the ratio of the major to minor semi-axes. (Peres-Rodrigues, 1966).

DATA SUMMARY

Table 2 contains the results of the ultrasonic velocity measurements including the calculated values of the dynamic shear modulus, dynamic Young's modulus as well as Poisson's ratio estimated on the basis of velocity data for each sample. As noted, an estimated Poisson's ratio of .25 was used in calculating the dynamic Young's moduli for borehole 101-S09-MOD1. This, as well as the inability to calculate the dynamic shear moduli for these samples, is due to a lack of shear wave velocity data.

Table 3 summarizes the uniaxial compression measurements which include loading rate, uniaxial compressive strength, tangent modulus of elasticity, secant modulus of elasticity, Poisson's ratio and the predominant mode of failure for each specimen.

Tables 4 through 6 include the most probable ellipsoid, rotation matrix and standard form equations of each borehole for uniaxial compressive strength, 50% secant modulus and 50% tangent modulus, respectively.

Table 7 contains the maximum anisotropies of the mechanical properties determined for each sample set as well as their means. As noted, the values determined for borehole #101-S09-MOD1 were not included in the mean calculations because of their dissimilar composition.

Table 8 summarizes the mean, standard deviation and spread of the anisotropy data for each of the uniaxial compressive strength, 50% secant and 50% tangent moduli of elasticity.

OBSERVATIONS AND CONCLUSIONS

The predominant modes of failure were those of a double wedge or cone configuration. These were accompanied by considerable axial splitting and slabbing with partially formed single diagonal failure planes being evident in several samples.

Paul and Gangal (1966) indicate that the double wedge or cone type failure is a result of end constraint generated by frictional forces acting between the specimen and platen surfaces. Samples prepared for this program, however, had sufficiently large length to diameter ratios (eg. 2 to 3:1) to minimize these effects at specimen mid-height where deformation readings were taken.

As Table 8 indicates, mean anisotropies of 1.54, 1.33 and 1.31 were determined for the uniaxial compressive strength, 50% secant and 50% tangent moduli, respectively. The standard deviation associated with the 50% secant modulus is 0.13 with values ranging from 1.16 to 1.50 and reflects a relatively consistent degree of anisotropy from hole to hole. Standard deviations of 0.35 and 0.25 calculated for the anisotropies of

the uniaxial compressive strength and 50% tangent modulus, however, are considerably higher and indicative of larger data spreads. An examination of a cumulative probability plot for the 50% tangent modulus of elasicity (see Figure 2), however, reveals that values determined for boreholes 001-041-MOD1, 206-012-MOD1 and 001-275-MOD2 do not belong to the same population as those of the remaining nine boreholes. A revised mean anisotropy of 1.18 is obtained if these are disregarded and indicates that, in terms of the 50% tangent modulus, the specimens tested are very nearly isotropic.

Many investigators have considered the effect of microstructure on the uniaxial mechanical properties of rock. Lama and Vutukuri (1978) state that the orientation of such features as bedding planes (schistosity, gneissicity etc.), mineral content and voids (pores, microcracks etc.) can profoundly affect the anisotropy of observed mechanical properties including the modulus of elasticity.

The 50% tangent modulus provides an estimate of the intrinsic modulus associated with the linear elastic zone of the uniaxial stress-strain curve and isn't, therefore, greatly influenced by microcracks in the specimen. Deformations measured during the early stages of loading, on the other hand, are greatly affected by crack closure and generally results in the secant modulus being smaller than its corresponding tangent modulus. The extent to which these pores and microcracks affect the initial deformation modulus is also often dependent upon their orientation with respect to the axis of loading. Cracks perpendicular to the loading axis tend to result in larger deformations during initial loading than those which are parallel to it. It follows that if a preferred orientation of microcracks exists in an otherwise nearly homogeneous rock mass, the secant modulus will exhibit a greater degree of anisotropy than that observed for the tangent modulus as is the case here.

The rather large variation in anisotropies from hole to hole can be attributed to utilizing only nine points to define a quadratic equation involving six unknowns. The condition exists, therefore, where one anomalous sample or instrument reading can have considerable impact on the calculated anisotropies. This problem may be alleviated, however, by rotating the results from all holes into a common coordinate system to provide a much larger population from which to perform the analyses. The subsequent ellipsoidal fit and rotation into standard form should yield a regional anisotropy for the properties determined as part of this program. In the case of the 50% secant modulus, the major semi-axis of the standard form will represent the largest predicted modulus. If this is the case, then the direction associated with the major semi-axis should coincide directly with the prevailing orientation of the microcracks if indeed one exists. Since the rotation matrix is comprised of direction cosines which transform the common coordinate system into one containing the standard form, its orientation in

space should be readily obtained. While beyond the scope of this report, future studies will employ the geographic orientation supplied by URL investigators to perform such analyses.

It may also prove useful to calculate the secant modulus at a lower stress level where the effect of crack closure and the consequent anisotropy will be more pronounced. A modulus determined by joining the origin to the stress-strain plot at 25 MPa is suggested so results can be compared with biaxial testing already in progress.

Table 1 : Summary of sample depth, dimensions, density and orientation

Drill Hole	Sample Depth	Length	Diameter	Density	Orientation	
	(m)	(mm)	(mm)	(gm/cc)	α	β
206-010-MOD1	3.130	113.80	44.42	2.66	90.0	0.0
	3.185	112.66	44.44	2.64	90.0	90.0
	3.243	110.80	44.42	2.64	90.0	45.0
	3.425	110.84	44.40	2.64	135.0	0.0
	3.570A	108.54	44.32	2.64	135.0	270.0
	3.570B	90.16	44.40	2.63	0.0	
	3.570C	111.64	44.34	2.64	0.0	
	3.774	82.38	44.38	2.64	135.0	270.0
	3.892	112.16	44.42	2.63	135.0	0.0
	3.979	109.74	44.50	2.64	90.0	315.0
	4.040	108.56	44.50	2.63	90.0	270.0
	4.102	106.80	44.46	2.64	90.0	0.0
206-012-MOD1	4.017	108.64	44.36	2.63	90.0	90.0
	4.077	111.04	44.38	2.64	90.0	60.0
	4.137	111.44	44.40	2.64	90.0	30.0
	4.197	109.42	44.50	2.62	90.0	0.0
	4.212	109.00	44.34	2.64	60.0	90.0
	4.337	112.50	44.40	2.64	60.0	0.0
	4.342	118.40	44.40	2.63	30.0	90.0
	4.492	113.00	44.40	2.65	30.0	0.0
	4.912	113.82	44.24	2.65	90.0	0.0

Table 1 : Continued

Drill Hole	Sample Depth	Length	Diameter	Density	Orientation	
	(m)	(mm)	(mm)	(gm/cc)	α	β
206-013-MOD1	4.190	111.40	44.44	2.64	0.0	
	4.282	111.83	44.50	2.63	30.0	0.0
	4.420	110.02	44.43	2.64	30.0	90.0
	4.657	111.07	44.42	2.64	60.0	0.0
	4.756	102.03	44.42	2.89	60.0	90.0
	4.892	112.46	44.46	2.64	90.0	0.0
	4.987	110.38	44.49	2.64	90.0	30.0
	5.002	110.49	44.44	2.65	90.0	60.0
	5.062	111.09	44.50	2.64	90.0	90.0
206-016-MOD1	5.252	112.36	44.52	2.64	0.0	
	5.342	111.12	44.52	2.66	30.0	0.0
	5.482	110.43	44.48	2.63	60.0	0.0
	5.717	112.22	44.48	2.64	60.0	90.0
	5.817	111.98	44.48	2.65	90.0	0.0
	5.952	113.60	44.52	2.66	90.0	30.0
	6.002	109.14	44.52	2.67	90.0	60.0
	6.052	109.19	44.48	2.68	90.0	60.0
	6.102	109.51	44.48	2.67	90.0	90.0

Table 1 : Continued

Drill Hole	Sample Depth	Length	Diameter	Density	Orientation	
	(m)	(mm)	(mm)	(gm/cc)	α	β
001-041-MOD1	2.060	105.14	44.48	2.63	0.0	
	2.152	99.76	44.32	2.62	30.0	0.0
	2.290	105.00	44.36	2.62	30.0	90.0
	2.527	110.79	44.44	2.62	60.0	0.0
	2.626	108.52	44.44	2.64	60.0	90.0
	2.751	109.97	44.50	2.63	90.0	0.0
	2.808	110.66	44.50	2.62	90.0	30.0
	2.862	110.10	44.50	2.62	90.0	60.0
	2.917	107.29	44.50	2.63	90.0	90.0
001-041-MOD2	2.475	106.35	44.46	2.64	0.0	
	2.565	112.96	44.48	2.63	30.0	0.0
	2.705	108.27	44.49	2.63	30.0	90.0
	2.938	111.87	44.44	2.63	60.0	0.0
	3.038	108.37	44.43	2.64	60.0	90.0
	3.170	108.24	44.44	2.63	90.0	0.0
	3.220	112.95	44.42	2.62	90.0	30.0
	3.270	101.05	44.50	2.89	90.0	60.0
	3.320	110.29	44.47	2.63	90.0	90.0

Table 1 : Continued

Drill Hole	Sample Depth	Length	Diameter	Density	Orientation	
	(m)	(mm)	(mm)	(gm/cc)	α	β
001-072-MOD1	1.290	114.49	44.58	2.63	90.0	30.0
	1.345	113.05	44.54	2.63	90.0	0.0
	1.395	111.99	44.54	2.64	90.0	60.0
	1.448	113.50	44.54	2.63	90.0	90.0
	1.460	112.70	44.54	2.63	60.0	0.0
	1.855	113.70	44.44	2.64	0.0	
	2.058	113.64	44.55	2.63	60.0	90.0
	2.158	113.38	44.58	2.63	30.0	90.0
	2.283	113.89	44.48	2.63	30.0	0.0
001-072-MOD2	1.497	112.88	44.54	2.62	90.0	0.0
	1.550	112.36	44.54	2.62	90.0	30.0
	1.604	113.48	44.54	2.62	90.0	60.0
	1.659	113.48	44.54	2.63	90.0	90.0
	1.667	113.64	44.58	2.63	60.0	0.0
	1.759	113.68	44.58	2.62	30.0	0.0
	2.132	113.70	44.47	2.62	0.0	
	2.215	113.26	44.58	2.62	60.0	90.0
	2.309	113.04	44.57	2.64	30.0	90.0

Table 1 : Continued

Drill Hole	Sample Depth	Length	Diameter	Density	Orientation	
	(m)	(mm)	(mm)	(gm/cc)	α	β
001-228-MOD1	3.414	112.79	44.50	2.63	90.0	0.0
	3.470	109.57	44.50	2.62	90.0	30.0
	3.525	112.05	44.49	2.62	90.0	60.0
	3.580	110.49	44.50	2.62	90.0	90.0
	3.590	112.18	44.52	2.62	60.0	0.0
	3.690	110.77	44.52	2.64	60.0	90.0
	3.695	113.60	44.52	2.64	30.0	0.0
	3.835	111.29	44.50	2.64	30.0	90.0
	4.180	110.27	44.48	2.63	0.0	
001-228-MOD2	3.488	108.69	44.50	2.63	90.0	0.0
	3.543	112.97	44.50	2.63	90.0	30.0
	3.598	108.05	44.50	2.64	90.0	60.0
	3.653	113.05	44.52	2.64	90.0	90.0
	3.674	112.72	44.50	2.64	60.0	0.0
	3.791	111.70	44.50	2.64	60.0	90.0
	3.791	112.27	44.54	2.64	30.0	0.0
	3.943	113.79	44.48	2.64	30.0	90.0
	4.342	112.71	44.50	2.64	0.0	

Table 1 : Continued

Drill Hole	Sample Depth	Length	Diameter	Density	Orientation	
	(m)	(mm)	(mm)	(gm/cc)	α	β
001-275-MOD1	1.850	113.87	44.49	2.64	90.0	0.0
	1.905	113.40	44.49	2.63	90.0	30.0
	1.960	111.27	44.48	2.64	90.0	60.0
	2.015	110.40	44.49	2.63	90.0	90.0
	2.033	113.41	44.52	2.63	60.0	0.0
	2.144	110.39	44.54	2.63	30.0	0.0
	2.146	111.91	44.52	2.63	60.0	90.0
	2.296	110.68	44.52	2.62	30.0	90.0
	2.715	112.20	44.46	2.63	0.0	
001-275-MOD2	1.852	112.82	44.50	2.64	90.0	0.0
	1.907	112.90	44.51	2.64	90.0	30.0
	1.962	112.76	44.50	2.64	90.0	60.0
	2.032	112.41	44.54	2.62	60.0	0.0
	2.145	112.70	44.56	2.63	30.0	0.0
	2.147	113.00	44.54	2.64	60.0	90.0
	2.294	113.86	44.55	2.62	30.0	90.0
	2.674	112.56	44.46	2.63	0.0	

Table 1 : Continued

Drill Hole	Sample Depth	Length	Diameter	Density	Orientation	
	(m)	(mm)	(mm)	(gm/cc)	α	β
101-S09-MOD1	3.489	103.88	44.46	2.70	0.0	axial
	4.190	104.28	44.42	2.98	90.0	0.0
	4.240	105.04	44.30	3.05	90.0	30.0
	4.290	104.44	44.32	2.70	90.0	60.0
	4.340	104.42	44.42	2.71	90.0	90.0
	3.580	105.14	44.22	2.62	30.0	0.0
	3.719	104.48	44.10	3.14	30.0	90.0
	3.955	104.38	44.30	2.90	60.0	0.0
	4.054	104.82	44.40	2.74	60.0	90.0
101-S02-MOD1	0.746	104.92	44.34	2.63	0.0	axial
	1.320	104.50	44.40	2.63	90.0	0.0
	1.250	105.32	44.38	2.63	90.0	30.0
	1.170	105.24	44.42	2.63	90.0	60.0
	1.045	99.68	44.42	2.63	90.0	90.0

Table 2 : Summary of ultrasonic velocity properties

Drill Hole	Sample Depth (m)	P-wave (km/sec)	S-wave (km/sec)	Dynamic Shear Modulus (GPa)	Dynamic Young's Modulus (GPa)	Poisson's ratio
206-010-MOD1	3.130	4.78	2.41	15.36	40.84	0.33
	3.185	3.87	2.40	15.20	36.10	0.19
	3.243	4.68	2.35	14.58	38.82	0.33
	3.425	4.55	3.42	30.87	52.51	-0.15
	3.570A	3.89	2.32	14.20	34.77	0.22
	3.570B	4.53	2.27	13.57	40.72	0.33
	3.570C	4.41	2.43	15.59	39.97	0.28
	3.774	3.92	2.11	11.75	30.47	0.30
	3.892	4.51	2.23	13.10	35.06	0.34
	3.979	4.23	2.05	11.09	29.87	0.35
	4.048	3.99	2.71	19.34	41.47	0.07
	4.102	5.02	2.66	18.64	48.65	0.30
206-012-MOD1	4.017	3.78	3.03	24.15	29.03	-0.40
	4.077	4.00	2.58	17.57	40.18	0.14
	4.137	4.44	2.31	14.08	37.02	0.31
	4.197	4.72	2.91	22.19	52.96	0.19
	4.212	3.61	2.75	19.99	32.33	-0.19
	4.337	4.70	2.84	21.25	51.54	0.21
	4.342	3.85	2.37	14.77	35.30	0.19
	4.492	4.37	2.41	15.37	39.40	0.28
	4.912	4.35	2.82	21.09	47.98	0.14

Table 2 : Continued

Drill Hole	Sample Depth (m)	P-wave (km/sec)	S-wave (km/sec)	Dynamic Shear Modulus (GPa)	Dynamic Young's Modulus (GPa)	Poisson's ratio
206-013-MOD1	4.190	4.39	3.20	27.03	50.45	-0.07
	4.282	4.52	3.31	28.81	53.12	-0.08
	4.420	4.02	2.97	23.29	41.87	-0.10
	4.657	4.79	3.39	30.34	60.57	-0.02
	4.756	3.46	2.65	20.30	32.09	-0.21
	4.892	4.80	3.44	31.24	60.73	-0.03
	4.947	4.83	3.47	31.79	61.46	-0.03
	5.002	4.40	3.24	27.82	50.50	-0.09
	5.062	3.94	2.99	23.60	38.76	-0.18
001-041-MOD2	2.475	3.98	2.84	21.29	41.79	-0.02
	2.565	4.19	3.19	26.76	43.39	-0.19
	2.705	4.22	2.74	19.74	44.84	0.14
	2.938	4.72	3.40	30.40	58.42	-0.04
	3.038	4.63	2.93	22.66	52.85	0.17
	3.170	4.92	3.40	30.40	63.42	0.04
	3.220	4.68	3.37	29.76	57.22	-0.04
	3.270	3.89	2.86	23.64	43.11	-0.09
	3.320	4.12	3.03	24.15	43.99	-0.09

Table 2 : Continued

Drill Hole	Sample Depth (m)	P-wave (km/sec)	S-wave (km/sec)	Dynamic Shear Modulus (GPa)	Dynamic Young's Modulus (GPa)	Poisson's ratio
001-072-MOD1	1.290	5.14	3.48	30.82	66.33	0.08
	1.345	5.58	3.65	33.91	76.34	0.13
	1.395	4.34	3.24	26.71	46.67	-0.13
	1.448	4.15	2.89	21.31	43.73	0.03
	1.460	5.54	3.61	33.07	74.86	0.13
	1.855	5.16	3.44	30.02	66.11	0.10
	2.058	4.26	2.62	17.46	41.76	0.20
	2.158	4.93	3.32	27.90	60.66	0.09
	2.283	5.42	3.57	32.37	72.36	0.12
001-072-MOD2	1.497	5.72	3.73	35.15	79.48	0.13
	1.550	5.23	3.48	30.76	67.66	0.10
	1.604	4.88	3.24	26.57	58.82	0.11
	1.659	4.82	3.31	27.89	58.65	0.05
	1.667	5.36	3.59	32.68	71.45	0.09
	1.759	4.71	2.93	21.81	51.57	0.18
	2.132	4.08	2.74	19.05	41.38	0.09
	2.215	4.98	3.35	28.36	61.71	0.09
	2.309	4.87	3.19	25.89	58.28	0.12

Table 2 : Continued

Drill Hole	Sample Depth (m)	P-wave (km/sec)	S-wave (km/sec)	Dynamic Shear Modulus (GPa)	Dynamic Young's Modulus (GPa)	Poisson's ratio
001-228-MOD1	3.414	5.85	3.82	36.99	83.54	0.13
	3.470	5.53	3.60	32.88	74.41	0.13
	3.525	5.20	3.40	27.27	65.92	0.13
	3.580	5.10	3.32	27.82	63.10	0.13
	3.590	5.51	3.57	32.31	73.53	0.14
	3.690	5.16	3.48	31.04	67.22	0.08
	3.695	5.15	3.59	32.92	67.72	0.03
	3.835	5.16	3.39	29.32	65.82	0.12
	4.180	5.12	3.51	31.37	66.17	0.06
001-228-MOD2	3.488	5.69	3.85	37.64	81.23	0.08
	3.543	5.81	3.86	37.81	83.65	0.11
	3.598	5.61	3.78	36.37	78.97	0.09
	3.653	5.42	3.75	35.77	74.53	0.04
	3.674	5.68	3.87	38.13	81.41	0.07
	3.791	5.41	3.70	34.86	73.97	0.06
	3.791	5.45	3.79	36.65	75.53	0.03
	3.943	5.30	3.69	34.77	71.56	0.03
	4.342	5.43	3.76	36.29	74.93	0.03

Table 2 : Continued

Drill Hole	Sample Depth (m)	P-wave (km/sec)	S-wave (km/sec)	Dynamic Shear Modulus (GPa)	Dynamic Young's Modulus (GPa)	Poisson's ratio
001-275-MOD1	1.850	5.35	3.58	32.64	71.35	0.09
	1.905	5.37	3.50	31.18	70.44	0.13
	1.960	5.16	3.47	30.61	66.72	0.09
	2.015	4.93	3.81	36.89	55.64	-0.25
	2.033	5.16	3.47	30.59	66.34	0.08
	2.144	4.86	3.26	26.64	57.98	0.09
	2.146	4.70	3.12	25.07	55.36	0.10
	2.296	4.70	3.63	33.48	50.60	-0.24
	2.715	4.63	3.20	26.03	54.18	0.04
001-275-MOD2	1.852	5.27	3.56	32.44	70.00	0.08
	1.907	5.39	3.60	33.09	72.57	0.10
	1.962	5.18	3.49	31.05	67.39	0.09
	2.032	5.25	3.50	31.06	68.34	0.10
	2.145	5.25	3.49	31.04	68.49	0.10
	2.147	4.88	3.37	28.96	60.42	0.04
	2.294	5.02	3.97	39.88	53.00	-0.33
	2.674	5.00	3.36	28.74	62.46	0.09

Table 2 : Continued

Drill Hole	Sample Depth (m)	P-wave (km/sec)	S-wave (km/sec)	Dynamic Shear Modulus (GPa)	Dynamic Young's Modulus (GPa)	Poisson's ratio
101-S09-MOD1	3.489	5.14	3.55	N.A.	59.49	0.25
	4.190	5.03	3.76	N.A.	62.91	0.25
	4.240	4.38	3.91	N.A.	48.79	0.25
	4.290	4.23	4.00	N.A.	40.21	0.25
	4.340	3.94	3.76	N.A.	35.02	0.25
	3.580	4.06	3.56	N.A.	36.11	0.25
	3.719	4.25	4.00	N.A.	47.18	0.25
	3.955	5.04	4.04	N.A.	61.16	0.25
	4.054	4.46	3.89	N.A.	45.27	0.25
101-S02-MOD1	0.746	5.22	3.48	31.89	70.15	0.10
	1.320	5.87	3.72	36.31	84.63	0.16
	1.250	5.71	3.65	35.02	80.87	0.15
	1.170	4.91	3.33	29.20	62.72	0.07
	1.045	4.27	2.86	21.47	46.95	0.09

Table 3 : Summary of Uniaxial Compression Properties

Drill Hole	Sample Depth (m)	Loading Rate (MPa/sec)	Uniaxial Compressive Strength (MPa)	Tangent Modulus of Elasticity (GPa)	Secant Modulus of Elasticity (GPa)	Poisson's ratio	Predominant Failure Characteristic
206-010-MOD1	3.130	0.65	174	68.99	57.81	0.24	double wedge
	3.185	0.73	215	64.50	45.05	0.23	double wedge
	3.243	0.86	164	67.33	57.80	0.26	double cone
	3.425	1.00	203	69.45	57.65	0.24	double cone
	3.570A	0.91	210	68.10	47.40	0.26	double wedge
	3.570B	0.92	185	64.94	50.55	0.23	double wedge
	3.570C	0.84	205	63.65	50.31	0.22	double wedge
	3.774	0.70	187	69.15	47.81	0.23	axial splitting
	3.892	0.78	168	65.01	51.18	0.24	bottom wedge
	3.979	0.83	165	66.85	54.60	0.20	bottom wedge
	4.048	1.07	204	71.55	49.65	0.24	double cone
	4.102	0.50	75	67.12	52.79	0.38	axial splitting
206-012-MOD1	4.017	0.72	192	61.81	42.33	0.21	bottom cone
	4.077	0.67	165	66.00	45.42	0.19	bottom cone
	4.137	0.81	184	65.37	53.47	0.20	double cone
	4.197	0.83	172	69.44	54.36	0.29	bottom cone
	4.212	0.80	189	63.56	41.74	0.19	double wedge
	4.337	0.89	179	62.51	51.58	0.23	double wedge
	4.342	0.93	198	59.91	44.45	0.29	bottom wedge
	4.492	0.51	75	40.22	13.57	N.A.	axial splitting
	4.912	0.90	191	63.15	48.89	0.25	double wedge

Table 3 : Continued

Drill Hole	Sample Depth (m)	Loading Rate (MPa/sec)	Uniaxial Compressive Strength (MPa)	Tangent Modulus of Elasticity (GPa)	Secant Modulus of Elasticity (GPa)	Poisson's Ratio	Predominant Failure Characteristic
206-013-MOD1	4.190	1.07	186	62.22	48.71	0.24	diagonal plane
	4.282	1.04	177	66.55	49.54	0.38	diagonal plane
	4.420	1.11	208	68.50	48.46	0.29	double wedge
	4.657	1.39	203	71.57	58.78	0.26	double wedge
	4.756	1.15	210	65.71	45.15	0.24	bottom wedge
	4.892	1.17	191	63.16	54.74	0.28	double wedge
	4.947	1.14	191	65.76	54.89	0.26	diagonal plane
	6.002	1.21	197	63.86	46.88	0.28	diagonal plane
	5.062	1.06	221	67.10	48.58	0.24	double wedge
206-016-MOD1	5.252	1.23	215	74.23	51.25	0.28	double wedge
	5.342	1.16	199	70.55	52.22	0.24	bottom wedge
	5.482	0.82	172	69.87	48.87	0.27	diagonal plane
	5.717	1.09	197	63.68	49.52	0.22	double wedge
	5.817	0.79	172	74.49	52.02	0.30	top wedge
	5.952	1.18	216	70.29	65.09	0.22	bottom wedge
	6.002	1.13	242	68.21	60.38	0.21	diagonal plane
	6.052	1.17	247	69.17	58.86	0.27	double wedge
	6.102	0.86	164	61.04	48.69	0.25	diagonal plane

Table 3 : Continued

Drill Hole	Sample Depth	Loading Rate (MPa/sec)	Uniaxial Compressive Strength (MPa)	Tangent Modulus of Elasticity (GPa)	Secant Modulus of Elasticity (GPa)	Poisson's Ratio	Predominant Failure Characteristic
001-041-MOD1	2.060	1.16	201	65.96	44.19	0.30	double cone
	2.152	0.99	170	69.40	45.18	0.25	double wedge
	2.290	0.95	176	55.63	36.12	0.30	diagonal plane
	2.527	0.90	168	59.53	41.86	0.29	double wedge
	2.626	0.86	120	48.87	42.39	0.23	bottom wedge
	2.751	0.90	174	63.81	48.38	0.29	double wedge
	2.808	0.78	127	63.85	52.74	0.35	double wedge
	2.862	1.08	187	64.02	45.15	0.22	double wedge
	2.917	1.17	185	60.42	38.00	0.24	double wedge
001-041-MOD2	2.475	0.98	210	62.86	41.88	0.24	double cone
	2.565	1.15	205	66.60	49.61	0.23	diagonal plane
	2.705	0.77	219	68.38	46.91	0.24	double wedge
	2.938	0.89	191	69.09	55.93	0.28	diagonal plane
	3.038	1.15	235	70.10	50.46	0.22	double wedge
	3.170	0.96	182	66.62	56.72	0.25	diagonal plane
	3.220	0.94	205	69.48	56.26	0.25	diagonal plane
	3.270	1.00	208	66.01	48.98	0.26	double wedge
	3.320	1.11	209	64.36	48.11	0.24	double wedge

Table 3 : Continued

Drill Hole	Sample Depth (m)	Loading Rate (MPa/sec)	Uniaxial Compressive Strength (MPa)	Tangent Modulus of Elasticity (GPa)	Secant Modulus of Elasticity (GPa)	Poisson's Ratio	Predominate Failure Characteristic
001-072-MOD1	1.290	1.20	174	65.08	55.49	0.26	diagonal plane
	1.345	0.90	194	71.53	68.31	0.29	diagonal plane
	1.395	0.56	142	68.63	61.76	0.22	diagonal plane
	1.448	0.76	191	64.04	47.87	0.20	double wedge
	1.460	0.81	151	64.90	66.30	0.17	diagonal plane
	1.855	1.02	196	66.48	58.49	0.22	double wedge
	2.058	0.94	179	65.65	54.56	0.27	double cone
	2.158	0.59	134	65.56	54.86	0.21	bottom wedge
	2.283	0.93	169	66.21	64.02	0.23	axial splitting
001-072-MOD2	1.497	0.68	166	68.92	66.08	0.25	double cone
	1.550	0.72	144	65.92	61.41	0.26	bottom wedge
	1.604	0.87	171	64.60	54.24	0.22	bottom cone
	1.659	0.88	198	68.46	58.89	0.30	bottom cone
	1.667	0.97	166	73.29	66.01	0.29	bottom wedge
	1.759	0.80	172	68.32	54.70	0.33	axial splitting
	2.132	0.79	194	65.88	50.27	0.21	double cone
	2.215	0.82	176	65.35	59.73	0.26	bottom wedge
	2.309	0.96	185	75.33	65.41	0.26	top wedge

Table 3 : Continued

Drill Hole	Sample Depth (m)	Loading Rate (MPa/sec)	Uniaxial Compressive Strength (MPa)	Tangent Modulus of Elasticity (GPa)	Secant Modulus of Elasticity (GPa)	Poisson's Ratio	Predominant Failure Characteristic
001-228-MOD1	3.414	0.98	194	70.32	69.69	0.24	double cone
	3.470	0.82	179	58.75	57.71	0.18	bottom cone
	3.525	1.10	179	70.61	65.10	0.26	double cone
	3.580	0.81	155	65.33	57.46	0.29	bottom wedge
	3.590	0.73	145	65.87	62.96	0.22	bottom wedge
	3.690	0.86	177	69.56	60.07	0.24	top wedge
	3.695	0.69	204	70.42	64.44	0.22	diagonal plane
	3.835	0.87	204	66.61	65.03	0.26	double cone
	4.180	0.80	198	69.89	63.79	0.27	top wedge
001-228-MOD2	3.488	1.16	228	73.46	71.96	0.25	double cone
	3.543	1.02	210	72.25	71.02	0.23	bottom wedge
	3.598	0.86	194	70.14	69.78	0.21	double wedge
	3.653	0.92	222	70.91	67.43	0.23	bottom cone
	3.674	0.90	215	77.25	74.97	0.26	double wedge
	3.791	0.96	201	69.54	64.35	0.20	double cone
	3.791	0.95	217	73.54	70.34	0.25	double cone
	3.943	0.88	219	69.63	65.28	0.24	double cone
	4.342	0.92	210	69.91	65.90	0.25	bottom wedge

Table 3 : Continued

Drill Hole	Sample Depth (m)	Loading Rate (MPa/sec)	Uniaxial Compressive Strength (MPa)	Tangent Modulus of Elasticity (GPa)	Secant Modulus of Elasticity (GPa)	Poisson's Ratio	Predominant Failure Characteristics
001-275-MOD1	1.850	1.11	167	68.50	64.12	0.25	bottom wedge
	1.905	0.98	192	68.44	63.72	0.28	double wedge
	1.960	0.99	180	77.76	68.59	0.25	bottom wedge
	2.015	1.08	174	70.16	61.52	0.27	bottom wedge
	2.033	0.98	192	74.70	69.03	0.30	bottom wedge
	2.144	0.98	146	66.36	56.05	0.28	diagonal plane
	2.146	0.88	202	71.01	64.66	0.25	double cone
	2.296	1.02	188	61.86	58.79	0.19	axial splitting
	2.715	0.86	206	66.22	56.96	0.21	double wedge
001-275-MOD2	1.852	0.81	172	71.19	64.73	0.23	double cone
	1.907	0.91	166	70.09	64.05	0.31	double cone
	1.962	0.85	158	77.41	57.50	0.23	discontinuity
	2.032	0.80	168	74.26	64.35	0.29	double cone
	2.145	0.90	162	74.21	66.68	0.26	double cone
	2.147	0.79	167	68.12	60.16	0.23	double cone
	2.294	0.66	186	65.08	60.03	0.21	double cone
	2.674	0.80	186	67.79	60.43	0.27	double cone

Table 3 : Continued

Drill Hole	Sample Depth (m)	Loading Rate (MPa/sec)	Uniaxial Compressive Strength (MPa)	Tangent Modulus of Elasticity (GPa)	Secant Modulus of Elasticity (GPa)	Poisson's Ratio	Predominant Failure Characteristic
101-S09-MOD1	3.489	0.75	133	73.90	60.69	0.20	axial splitting
	4.190	0.75	213	99.45	103.50	0.22	axial splitting
	4.240	0.75	232	107.80	113.70	0.80	axial splitting
	4.290	0.75	206	83.29	79.41	0.25	axial splitting
	4.340	0.75	163	76.71	67.09	0.23	axial splitting
	3.580	0.75	165	72.62	56.08	0.22	axial splitting
	3.791	0.75	158	84.83	98.09	0.20	axial splitting
	3.955	0.75	188	74.98	72.71	0.19	axial splitting
	4.054	0.75	198	71.57	65.25	0.22	axial splitting
101-S02-MOD1	0.746	0.75	152	69.45	59.03	0.23	diagonal plane
	1.320	0.75	156	76.47	72.84	0.34	axial splitting
	1.250	0.75	141	70.01	66.28	0.20	axial splitting
	1.170	0.75	164	72.41	59.13	0.25	axial splitting
	1.045	0.75	190	68.20	53.84	0.19	axial splitting

TABLE 4 :UNIAXIAL COMPRESSIVE STRENGTH : ELLIPSOIDAL FIT & ROTATION INTO STANDARD FORM

BOREHOLE # 206-010-MOD1

MOST PROBABLE ELLIPSOID	ROTATION MATRIX	NORMAL EQUATION
$(X\ Y\ Z)\begin{pmatrix}+2.3559 & +0.0171 & +0.0203\\ +0.0171 & +4.1339 & +0.5817\\ +0.0203 & +0.5817 & +2.5958\end{pmatrix}\begin{pmatrix}X\\Y\\Z\end{pmatrix}=10^5$	$\begin{pmatrix}+0.9623 & +0.0760 & -0.2611\\ -0.2717 & +0.3092 & -0.2611\\ -0.0115 & -0.9479 & -0.3182\end{pmatrix}$	$\frac{x^2}{206^2}+\frac{y^2}{204^2}+\frac{z^2}{152^2}=1$

BOREHOLE # 206-012-MOD1

MOST PROBABLE ELLIPSOID	ROTATION MATRIX	NORMAL EQUATION
$(X\ Y\ Z)\begin{pmatrix}+2.9798 & +0.3918 & -0.8203\\ +0.3918 & +2.8301 & +0.5657\\ -0.8203 & +0.5657 & +3.7332\end{pmatrix}\begin{pmatrix}X\\Y\\Z\end{pmatrix}=10^5$	$\begin{pmatrix}+0.6200 & +0.7691 & +0.1554\\ -0.4685 & +0.2040 & +0.8596\\ -0.6294 & +0.6057 & -0.4867\end{pmatrix}$	$\frac{x^2}{175^2}+\frac{y^2}{152^2}+\frac{z^2}{225^2}=1$

BOREHOLE # 206-013-MOD1

MOST PROBABLE ELLIPSOID	ROTATION MATRIX	NORMAL EQUATION
$(X\ Y\ Z)\begin{pmatrix}+2.1264 & +0.3534 & -0.2595\\ +0.3534 & +2.5833 & -0.0199\\ -0.2595 & -0.0199 & +2.906\end{pmatrix}\begin{pmatrix}X\\Y\\Z\end{pmatrix}=10^5$	$\begin{pmatrix}-0.3044 & -0.8336 & -0.4609\\ +0.3792 & +0.3378 & -0.8614\\ -0.8738 & +0.4370 & -0.2133\end{pmatrix}$	$\frac{x^2}{192^2}+\frac{y^2}{182^2}+\frac{z^2}{230^2}=1$

BOREHOLE # 206-016-MOD1

MOST PROBABLE ELLIPSOID	ROTATION MATRIX	NORMAL EQUATION
$(X\ Y\ Z)\begin{pmatrix}+3.0536 & -1.1809 & +0.8656\\ -1.1809 & +2.3207 & +0.3312\\ +0.8656 & +0.3312 & +2.2076\end{pmatrix}\begin{pmatrix}X\\Y\\Z\end{pmatrix}=10^5$	$\begin{pmatrix}+0.8184 & -0.4955 & +0.2912\\ -0.0919 & -0.6130 & -0.7847\\ -0.5673 & -0.6154 & +0.5472\end{pmatrix}$	$\frac{x^2}{157^2}+\frac{y^2}{197^2}+\frac{z^2}{327^2}=1$

TABLE 4: CONT'D

BOREHOLE # 001-041-MOD1

MOST PROBABLE ELLIPSOID

$$(X\ Y\ Z)\begin{pmatrix}+2.8964 & +0.3822 & +1.5563\\ +0.3822 & +3.5427 & +0.6431\\ +1.5563 & +0.6431 & +2.3587\end{pmatrix}\begin{pmatrix}X\\Y\\Z\end{pmatrix}=10^5$$

ROTATION MATRIX

$$\begin{pmatrix}+0.4775 & -0.8354 & +0.2722\\ -0.6197 & -0.5398 & -0.5698\\ -0.6229 & -0.1034 & +0.7754\end{pmatrix}$$

NORMAL EQUATION

$$\frac{x^2}{179^2}+\frac{y^2}{146^2}+\frac{z^2}{313^2}=1$$

BOREHOLE # 001-041-MOD2

MOST PROBABLE ELLIPSOID

$$(X\ Y\ Z)\begin{pmatrix}+2.2693 & -0.2903 & -0.4293\\ -0.2903 & +2.9320 & -0.0904\\ -0.4293 & -0.0904 & +2.3363\end{pmatrix}\begin{pmatrix}X\\Y\\Z\end{pmatrix}=10^5$$

ROTATION MATRIX

$$\begin{pmatrix}+0.4079 & -0.9036 & -0.1309\\ -0.5414 & -0.3549 & +0.7622\\ +0.7351 & +0.2400 & +0.6340\end{pmatrix}$$

NORMAL EQUATION

$$\frac{x^2}{181^2}+\frac{y^2}{193^2}+\frac{z^2}{235^2}=1$$

BOREHOLE # 001-072-MOD1

MOST PROBABLE ELLIPSOID

$$(X\ Y\ Z)\begin{pmatrix}+2.6871 & +1.3578 & +1.1690\\ +1.3578 & +2.6015 & +1.3700\\ +1.1690 & +1.3700 & +2.3363\end{pmatrix}\begin{pmatrix}X\\Y\\Z\end{pmatrix}=10^5$$

ROTATION MATRIX

$$\begin{pmatrix}+0.4111 & -0.8097 & +0.4187\\ +0.7112 & -0.0024 & -0.7030\\ -0.5702 & -0.5868 & -0.5749\end{pmatrix}$$

NORMAL EQUATION

$$\frac{x^2}{288^2}+\frac{y^2}{256^2}+\frac{z^2}{138^2}=1$$

BOREHOLE # 001-072-MOD2

MOST PROBABLE ELLIPSOID

$$(X\ Y\ Z)\begin{pmatrix}+2.5356 & +0.9991 & +0.5467\\ +0.9991 & +3.7059 & +0.3992\\ +0.5467 & +0.3992 & +2.6323\end{pmatrix}\begin{pmatrix}X\\Y\\Z\end{pmatrix}=10^5$$

ROTATION MATRIX

$$\begin{pmatrix}+0.8414 & -0.3660 & -0.3975\\ -0.2022 & +0.4689 & -0.8598\\ -0.5011 & -0.8038 & -0.3206\end{pmatrix}$$

NORMAL EQUATION

$$\frac{x^2}{233^2}+\frac{y^2}{198^2}+\frac{z^2}{149^2}=1$$

TABLE 4: CONT'D

BOREHOLE # 001-228-MOD1

MOST PROBABLE ELLIPSOID

$$(X\ Y\ Z)\begin{pmatrix}+3.9410 & -0.4000 & -0.3835\\ -0.4000 & +2.9937 & +0.3720\\ -0.3835 & +0.3720 & +2.3236\end{pmatrix}\begin{pmatrix}X\\Y\\Z\end{pmatrix}=10^5$$

ROTATION MATRIX

$$\begin{pmatrix}+0.4321 & +0.8619 & +0.2653\\ +0.1207 & -0.3468 & +0.9301\\ -0.8937 & +0.3699 & +0.2539\end{pmatrix}$$

NORMAL EQUATION

$$\frac{x^2}{185^2}+\frac{y^2}{216^2}+\frac{z^2}{154^2}=1$$

BOREHOLE # 001-228-MOD2

MOST PROBABLE ELLIPSOID

$$(X\ Y\ Z)\begin{pmatrix}+2.1497 & +0.4732 & +0.1233\\ +0.4732 & +1.9127 & +0.1382\\ +0.1233 & +0.1382 & +2.1322\end{pmatrix}\begin{pmatrix}X\\Y\\Z\end{pmatrix}=10^5$$

ROTATION MATRIX

$$\begin{pmatrix}+0.6054 & -0.7937 & +0.0593\\ -0.3277 & -0.1806 & +0.9274\\ +0.7253 & +0.5809 & +0.3694\end{pmatrix}$$

NORMAL EQUATION

$$\frac{x^2}{254^2}+\frac{y^2}{220^2}+\frac{z^2}{196^2}=1$$

BOREHOLE # 001-275-MOD1

MOST PROBABLE ELLIPSOID

$$(X\ Y\ Z)\begin{pmatrix}+3.1585 & -0.2320 & -0.3739\\ -0.2320 & +3.0043 & +0.3758\\ -0.3739 & +0.3758 & +2.6812\end{pmatrix}\begin{pmatrix}X\\Y\\Z\end{pmatrix}=10^5$$

ROTATION MATRIX

$$\begin{pmatrix}+0.6783 & +0.7257 & +0.1149\\ +0.2919 & -0.4097 & +0.8643\\ -0.6743 & +0.5809 & +0.4897\end{pmatrix}$$

NORMAL EQUATION

$$\frac{x^2}{187^2}+\frac{y^2}{205^2}+\frac{z^2}{166^2}=1$$

BOREHOLE # 001-275-MOD2

MOST PROBABLE ELLIPSOID

$$(X\ Y\ Z)\begin{pmatrix}+4.2192 & +0.0700 & -0.4059\\ +0.0700 & +3.3023 & +0.6186\\ -0.4059 & +0.6186 & +2.9475\end{pmatrix}\begin{pmatrix}X\\Y\\Z\end{pmatrix}=10^5$$

ROTATION MATRIX

$$\begin{pmatrix}-0.9355 & +0.1310 & +0.3281\\ +0.2907 & +0.8132 & +0.5043\\ +2.008 & -0.5671 & +0.7988\end{pmatrix}$$

NORMAL EQUATION

$$\frac{x^2}{152^2}+\frac{y^2}{164^2}+\frac{z^2}{204^2}=1$$

TABLE 4: CONT'D

BOREHOLE # 101-S09-MOD1

MOST PROBABLE ELLIPSOID

$$(X \;\; Y \;\; Z)\begin{pmatrix} +3.5262 & -0.9250 & -1.5213 \\ -0.9250 & +2.3152 & -0.6267 \\ -1.5213 & -0.6267 & +5.4585 \end{pmatrix}\begin{pmatrix} X \\ Y \\ Z \end{pmatrix} = 10^5$$

ROTATION MATRIX

$$\begin{pmatrix} +0.6816 & -0.6448 & +0.3459 \\ -0.5577 & -0.7638 & -0.3249 \\ -0.4737 & -0.0285 & +0.8802 \end{pmatrix}$$

NORMAL EQUATION

$$\frac{x^2}{166^2} + \frac{y^2}{270^2} + \frac{z^2}{126^2} = 1$$

TABLE 5 : 50% SECANT MODULUS OF ELASTICITY : ELLIPSOIDAL FIT & ROTATION INTO STANDARD FORM

BOREHOLE # 206-010-MOD1

MOST PROBABLE ELLIPSOID

$$(X\ Y\ Z)\begin{pmatrix}+40.5213 & -2.2986 & +4.2014\\ -2.2986 & +30.4492 & +1.6969\\ +4.2014 & +1.6969 & +39.3197\end{pmatrix}\begin{pmatrix}X\\Y\\Z\end{pmatrix}=10^5$$

ROTATION MATRIX

$$\begin{pmatrix}+0.2885 & +0.9174 & -0.2741\\ +0.5759 & -0.3950 & -0.7158\\ +0.7649 & -0.0486 & +0.6423\end{pmatrix}$$

NORMAL EQUATIONS

$$\frac{x^2}{58.50^2}+\frac{y^2}{52.08^2}+\frac{z^2}{47.57^2}=1$$

BOREHOLE # 206-012-MOD1

MOST PROBABLE ELLIPSOID

$$(X\ Y\ Z)\begin{pmatrix}+59.2522 & -7.3140 & -10.1306\\ -7.3140 & +36.2369 & -4.0651\\ -10.1306 & -4.0651 & +65.0875\end{pmatrix}\begin{pmatrix}X\\Y\\Z\end{pmatrix}=10^5$$

ROTATION MATRIX

$$\begin{pmatrix}+0.3347 & +0.9165 & +0.2190\\ +0.7167 & -0.3985 & +0.5723\\ -0.6118 & +0.0346 & +0.7902\end{pmatrix}$$

NORMAL EQUATIONS

$$\frac{x^2}{55.39^2}+\frac{y^2}{42.55^2}+\frac{z^2}{37.07^2}=1$$

BOREHOLE # 206-013-MOD1

MOST PROBABLE ELLIPSOID

$$(X\ Y\ Z)\begin{pmatrix}+45.0528 & +0.5039 & +1.5855\\ +0.5039 & +31.1323 & -3.7143\\ +1.5855 & -3.7143 & +43.0683\end{pmatrix}\begin{pmatrix}X\\Y\\Z\end{pmatrix}=10^5$$

ROTATION MATRIX

$$\begin{pmatrix}+0.8152 & -0.1136 & +0.5679\\ +0.5759 & +0.2633 & -0.7740\\ +0.0616 & -0.9580 & -0.2801\end{pmatrix}$$

NORMAL EQUATIONS

$$\frac{x^2}{46.58^2}+\frac{y^2}{48.14^2}+\frac{z^2}{57.72^2}=1$$

BOREHOLE # 206-016-MOD1

MOST PROBABLE ELLIPSOID

$$(X\ Y\ Z)\begin{pmatrix}+37.9227 & -3.8988 & +1.8970\\ -3.8988 & +25.3703 & +8.1342\\ +1.8970 & +8.1342 & +36.9446\end{pmatrix}\begin{pmatrix}X\\Y\\Z\end{pmatrix}=10^5$$

ROTATION MATRIX

$$\begin{pmatrix}+0.9706 & -0.1893 & +0.1487\\ +0.0444 & -0.4665 & -0.8834\\ -0.2366 & -0.8640 & +0.4444\end{pmatrix}$$

NORMAL EQUATIONS

$$\frac{x^2}{50.65^2}+\frac{y^2}{49.30^2}+\frac{z^2}{70.50^2}=1$$

TABLE 5 : CONT'D

BOREHOLE # 001-041-MOD1

MOST PROBABLE ELLIPSOID

$$(X\ Y\ Z)\begin{pmatrix}+63.9821 & -13.7391 & +4.7509\\ -13.7391 & +43.8995 & +5.0019\\ +4.7509 & +5.0019 & +51.6827\end{pmatrix}\begin{pmatrix}X\\Y\\Z\end{pmatrix}=10^5$$

ROTATION MATRIX

$$\begin{pmatrix}+0.8957 & -0.4315 & +0.1076\\ -0.0662 & -0.3687 & -0.9272\\ -0.4397 & -0.8233 & +0.3588\end{pmatrix}$$

NORMAL EQUATIONS

$$\frac{x^2}{37.48^2}+\frac{y^2}{43.03^2}+\frac{z^2}{53.93^2}=1$$

BOREHOLE # 001-041-MOD2

MOST PROBABLE ELLIPSOID

$$(X\ Y\ Z)\begin{pmatrix}+44.2313 & -1.7229 & -8.5727\\ -1.7229 & +31.0801 & -7.4567\\ -8.5727 & -7.4567 & +55.2379\end{pmatrix}\begin{pmatrix}X\\Y\\Z\end{pmatrix}=10^5$$

ROTATION MATRIX

$$\begin{pmatrix}+0.8624 & -0.3782 & +0.3364\\ -0.2680 & -0.9050 & -0.3303\\ -0.4294 & -0.1947 & +0.8819\end{pmatrix}$$

NORMAL EQUATIONS

$$\frac{x^2}{49.00^2}+\frac{y^2}{59.92^2}+\frac{z^2}{40.47^2}=1$$

BOREHOLE # 001-072-MOD1

MOST PROBABLE ELLIPSOID

$$(X\ Y\ Z)\begin{pmatrix}+35.6477 & -1.6796 & +1.1184\\ -1.6796 & +23.3379 & -3.0968\\ +1.1184 & -3.0968 & +29.2662\end{pmatrix}\begin{pmatrix}X\\Y\\Z\end{pmatrix}=10^5$$

ROTATION MATRIX

$$\begin{pmatrix}+0.9555 & -0.1804 & +0.2334\\ -0.2833 & -0.3407 & +0.8965\\ -0.0822 & -0.9227 & +0.3767\end{pmatrix}$$

NORMAL EQUATIONS

$$\frac{x^2}{52.53^2}+\frac{y^2}{57.65^2}+\frac{z^2}{67.54^2}=1$$

BOREHOLE # 001-072-MOD2

MOST PROBABLE ELLIPSOID

$$(X\ Y\ Z)\begin{pmatrix}+30.7402 & +4.0722 & -9.9946\\ +4.0722 & +21.9635 & -1.2937\\ -9.9946 & -1.9237 & +36.6091\end{pmatrix}\begin{pmatrix}X\\Y\\Z\end{pmatrix}=10^5$$

ROTATION MATRIX

$$\begin{pmatrix}+0.5094 & -0.8346 & +0.2094\\ -0.6132 & -0.5228 & -0.5921\\ -0.6037 & -0.1733 & +0.7782\end{pmatrix}$$

NORMAL EQUATIONS

$$\frac{x^2}{70.98^2}+\frac{y^2}{63.81^2}+\frac{z^2}{47.25^2}=1$$

TABLE 5 : CONT'D

BOREHOLE # 001-228-MOD1

MOST PROBABLE ELLIPSOID

$$(X\ Y\ Z)\begin{pmatrix} +28.0184 & +0.6555 & -0.3698 \\ +0.6555 & +22.2663 & +1.8901 \\ -0.3698 & +1.8901 & +23.6830 \end{pmatrix}\begin{pmatrix} X \\ Y \\ Z \end{pmatrix} = 10^5$$

ROTATION MATRIX

$$\begin{pmatrix} +0.9943 & +0.0984 & -0.0411 \\ +0.0219 & -0.5562 & -0.8240 \\ +0.1044 & -0.8184 & +0.5651 \end{pmatrix}$$

NORMAL EQUATIONS

$$\frac{x^2}{59.66^2} + \frac{y^2}{63.26^2} + \frac{z^2}{69.21^2} = 1$$

BOREHOLE # 001-228-MOD2

MOST PROBABLE ELLIPSOID

$$(X\ Y\ Z)\begin{pmatrix} +22.0437 & -0.5588 & +1.4812 \\ -0.5588 & +19.3104 & -2.5143 \\ +1.4812 & -2.5143 & +22.9732 \end{pmatrix}\begin{pmatrix} X \\ Y \\ Z \end{pmatrix} = 10^5$$

ROTATION MATRIX

$$\begin{pmatrix} +0.8858 & +0.2521 & -0.3897 \\ +0.0479 & -0.8847 & -0.4637 \\ +0.4616 & -0.3921 & +0.7957 \end{pmatrix}$$

NORMAL EQUATIONS

$$\frac{x^2}{68.63^2} + \frac{y^2}{74.49^2} + \frac{z^2}{63.16^2} = 1$$

BOREHOLE # 001-275-MOD1

MOST PROBABLE ELLIPSOID

$$(X\ Y\ Z)\begin{pmatrix} +24.9479 & -2.1474 & -3.1462 \\ -2.1474 & +24.1011 & -4.0140 \\ -3.1462 & -4.0140 & +33.1841 \end{pmatrix}\begin{pmatrix} X \\ Y \\ Z \end{pmatrix} = 10^5$$

ROTATION MATRIX

$$\begin{pmatrix} +0.7795 & -0.6264 & -0.0096 \\ -0.5851 & -0.7225 & -0.3684 \\ -0.2238 & -0.2927 & +0.9296 \end{pmatrix}$$

NORMAL EQUATIONS

$$\frac{x^2}{61.19^2} + \frac{y^2}{70.16^2} + \frac{z^2}{53.30^2} = 1$$

BOREHOLE # 001-275-MOD2

MOST PROBABLE ELLIPSOID

$$(X\ Y\ Z)\begin{pmatrix} +31.3571 & -0.8334 & -1.6782 \\ -0.8334 & +24.2191 & -2.7206 \\ -1.6782 & -2.7206 & +26.9198 \end{pmatrix}\begin{pmatrix} X \\ Y \\ Z \end{pmatrix} = 10^5$$

ROTATION MATRIX

$$\begin{pmatrix} +0.9460 & +0.0121 & -0.3240 \\ +0.2729 & -0.5692 & +0.7756 \\ +0.1750 & +0.8221 & +0.5417 \end{pmatrix}$$

NORMAL EQUATIONS

$$\frac{x^2}{55.97^2} + \frac{y^2}{59.42^2} + \frac{z^2}{67.04^2} = 1$$

TABLE 5 : CONT'D

BOREHOLE # 101-S09-MOD1

MOST PROBABLE ELLIPSOID

$$(X \;\; Y \;\; Z)\begin{pmatrix} +26.1518 & -6.6538 & -12.9199 \\ -6.6538 & +9.1876 & +9.2591 \\ -12.9199 & +9.2591 & +22.5215 \end{pmatrix}\begin{pmatrix} X \\ Y \\ Z \end{pmatrix} = 10^5$$

ROTATION MATRIX

$$\begin{pmatrix} -0.0026 & -0.8908 & +0.4544 \\ +0.7205 & +0.3135 & +0.6186 \\ +0.6935 & -0.3290 & -0.6410 \end{pmatrix}$$

NORMAL EQUATIONS

$$\frac{x^2}{149.99^2} + \frac{y^2}{90.67^2} + \frac{z^2}{49.24^2} = 1$$

TABLE 6 : 50 % TANGENT MODULUS OF ELASTICITY : ELLIPSOIDAL FIT & ROTATION INTO STANDARD FORM

BOREHOLE # 206-010-MOD1

MOST PROBABLE ELLIPSOID

$$(X\ Y\ Z)\begin{pmatrix}+21.5688 & -0.1514 & -1.6456\\ -0.1514 & +21.8183 & +0.9938\\ -0.6456 & +0.9938 & +24.1784\end{pmatrix}\begin{pmatrix}X\\Y\\Z\end{pmatrix}=10^5$$

ROTATION MATRIX

$$\begin{pmatrix}+0.3948 & +0.9131 & -0.1016\\ +0.8259 & -0.3242 & +0.4727\\ -0.402 & +0.2714 & +0.8742\end{pmatrix}$$

NORMAL EQUATION

$$\frac{x^2}{67.97^2}+\frac{y^2}{69.54^2}+\frac{z^2}{62.94^2}=1$$

BOREHOLE # 206-012-MOD1

MOST PROBABLE ELLIPSOID

$$(X\ Y\ Z)\begin{pmatrix}+27.0480 & -1.6855 & -12.3398\\ -1.6855 & +22.1746 & +0.5060\\ -12.3398 & +0.5060 & +47.7951\end{pmatrix}\begin{pmatrix}X\\Y\\Z\end{pmatrix}=10^5$$

ROTATION MATRIX

$$\begin{pmatrix}-0.5227 & +0.8061 & -0.2776\\ +0.7400 & +0.5906 & +0.3217\\ -0.4233 & +0.0373 & +0.9052\end{pmatrix}$$

NORMAL EQUATION

$$\frac{x^2}{65.80^2}+\frac{y^2}{70.12^2}+\frac{z^2}{43.20^2}=1$$

BOREHOLE # 206-013-MOD1

MOST PROBABLE ELLIPSOID

$$(X\ Y\ Z)\begin{pmatrix}+23.3185 & +0.2225 & -2.7284\\ +0.2225 & +23.8452 & -4.4375\\ -2.7284 & -4.4375 & +25.6297\end{pmatrix}\begin{pmatrix}X\\Y\\Z\end{pmatrix}=10^5$$

ROTATION MATRIX

$$\begin{pmatrix}+0.8450 & -0.5341 & -0.0273\\ -0.4226 & -0.6355 & -0.6462\\ -0.3278 & -0.5576 & +0.7627\end{pmatrix}$$

NORMAL EQUATION

$$\frac{x^2}{65.56^2}+\frac{y^2}{71.65^2}+\frac{z^2}{57.69^2}=1$$

BOREHOLE # 206-016-MOD1

MOST PROBABLE ELLIPSOID

$$(X\ Y\ Z)\begin{pmatrix}+23.7178 & -1.5502 & -2.6316\\ -1.5502 & +21.3113 & +2.3468\\ -2.6316 & +2.3468 & +18.7143\end{pmatrix}\begin{pmatrix}X\\Y\\Z\end{pmatrix}=10^5$$

ROTATION MATRIX

$$\begin{pmatrix}+0.5738 & +0.7988 & +0.1810\\ +0.2561 & -0.3849 & +0.8867\\ -0.7780 & +0.4264 & +0.4254\end{pmatrix}$$

NORMAL EQUATION

$$\frac{x^2}{69.46^2}+\frac{y^2}{76.84^2}+\frac{z^2}{61.92^2}=1$$

TABLE 6 : CONT'D

BOREHOLE # 001-041-MOD1

MOST PROBABLE ELLIPSOID

$$(X\ Y\ Z)\begin{pmatrix}+27.9037 & -2.9157 & +13.5067\\ -2.9157 & +26.0686 & +0.0607\\ +13.5067 & +0.0607 & +21.3008\end{pmatrix}\begin{pmatrix}X\\Y\\Z\end{pmatrix}=10^5$$

ROTATION MATRIX

$$\begin{pmatrix}-0.0641 & -0.9774 & -0.2014\\ -0.7815 & +0.1747 & -0.5989\\ -0.6206 & -0.1191 & +0.7750\end{pmatrix}$$

NORMAL EQUATION

$$\frac{x^2}{62.15^2}+\frac{y^2}{50.70^2}+\frac{z^2}{97.70^2}=1$$

BOREHOLE # 001-041-MOD2

MOST PROBABLE ELLIPSOID

$$(X\ Y\ Z)\begin{pmatrix}+24.3427 & -1.7462 & -4.6674\\ -1.7462 & +22.2262 & -2.4259\\ -4.6774 & -2.4259 & +25.4719\end{pmatrix}\begin{pmatrix}X\\Y\\Z\end{pmatrix}=10^5$$

ROTATION MATRIX

$$\begin{pmatrix}+0.5006 & -0.8075 & +0.3199\\ -0.6369 & -0.0996 & +0.7645\\ +0.5863 & +0.5813 & +0.5642\end{pmatrix}$$

NORMAL EQUATION

$$\frac{x^2}{64.22^2}+\frac{y^2}{58.04^2}+\frac{z^2}{74.31^2}=1$$

BOREHOLE # 001-072-MOD1

MOST PROBABLE ELLIPSOID

$$(X\ Y\ Z)\begin{pmatrix}+23.1637 & +0.4204 & +0.5704\\ +0.4204 & +20.5602 & +2.0816\\ +0.5704 & +2.0816 & +22.3153\end{pmatrix}\begin{pmatrix}X\\Y\\Z\end{pmatrix}=10^5$$

ROTATION MATRIX

$$\begin{pmatrix}+0.8222 & -0.3079 & -0.4787\\ -0.5691 & -0.4580 & -0.6829\\ +0.0090 & -0.8339 & +0.5518\end{pmatrix}$$

NORMAL EQUATION

$$\frac{x^2}{66.41^2}+\frac{y^2}{64.30^2}+\frac{z^2}{72.20^2}=1$$

BOREHOLE # 001-072-MOD2

MOST PROBABLE ELLIPSOID

$$(X\ Y\ Z)\begin{pmatrix}+22.7447 & +2.1453 & -3.0296\\ +2.1453 & +20.5212 & -1.6173\\ -3.0296 & -1.6173 & +22.0352\end{pmatrix}\begin{pmatrix}X\\Y\\Z\end{pmatrix}=10^5$$

ROTATION MATRIX

$$\begin{pmatrix}+0.6787 & -0.6457 & +0.3498\\ -0.2462 & -0.6489 & -0.7199\\ -0.6919 & -0.4025 & +0.5994\end{pmatrix}$$

NORMAL EQUATION

$$\frac{x^2}{72.28^2}+\frac{y^2}{71.54^2}+\frac{z^2}{61.29^2}=1$$

TABLE 6 : CONT'D

BOREHOLE # 001-228-MOD1

MOST PROBABLE ELLIPSOID

$$(X\ Y\ Z)\begin{pmatrix}+20.964 & +1.7705 & +0.9147\\ +1.7705 & +22.0570 & +0.2310\\ +0.9147 & +0.2310 & +20.4781\end{pmatrix}\begin{pmatrix}X\\Y\\Z\end{pmatrix}=10^5$$

ROTATION MATRIX

$$\begin{pmatrix}-0.7474 & +0.4397 & +0.4980\\ +0.2735 & -0.4795 & +0.8338\\ -0.6055 & -0.7594 & -0.2381\end{pmatrix}$$

NORMAL EQUATION

$$\frac{x^2}{71.96^2}+\frac{y^2}{69.60^2}+\frac{z^2}{65.18^2}=1$$

BOREHOLE # 001-228-MOD2

MOST PROBABLE ELLIPSOID

$$(X\ Y\ Z)\begin{pmatrix}+20.0392 & +0.6498 & +0.3948\\ +0.6498 & +18.3011 & -2.1317\\ +0.3948 & -2.1317 & +20.5807\end{pmatrix}\begin{pmatrix}X\\Y\\Z\end{pmatrix}=10^5$$

ROTATION MATRIX

$$\begin{pmatrix}+0.9728 & +0.1999 & +0.1166\\ -0.0027 & +0.5137 & -0.8580\\ +0.2314 & -0.8344 & -0.5003\end{pmatrix}$$

NORMAL EQUATION

$$\frac{x^2}{70.32^2}+\frac{y^2}{67.64^2}+\frac{z^2}{77.05^2}=1$$

BOREHOLE # 001-275-MOD1

MOST PROBABLE ELLIPSOID

$$(X\ Y\ Z)\begin{pmatrix}+18.7074 & -1.1837 & +1.0044\\ -1.8317 & +21.4990 & -3.6007\\ +1.0044 & -3.6007 & +24.6164\end{pmatrix}\begin{pmatrix}X\\Y\\Z\end{pmatrix}=10^5$$

ROTATION MATRIX

$$\begin{pmatrix}+0.8182 & +0.5501 & +0.1671\\ +0.5349 & -0.6218 & -0.5720\\ +0.2107 & -0.5574 & +0.8031\end{pmatrix}$$

NORMAL EQUATION

$$\frac{x^2}{75.21^2}+\frac{y^2}{71.13^2}+\frac{z^2}{60.44^2}=1$$

BOREHOLE # 001-275-MOD2

MOST PROBABLE ELLIPSOID

$$(X\ Y\ Z)\begin{pmatrix}+14.5574 & +1.2567 & +5.4586\\ +1.2567 & +20.1378 & -2.9511\\ +5.4586 & -2.9511 & +21.2665\end{pmatrix}\begin{pmatrix}X\\Y\\Z\end{pmatrix}=10^5$$

ROTATION MATRIX

$$\begin{pmatrix}+0.4239 & +0.8785 & +0.2206\\ -0.3831 & +0.3946 & -0.8352\\ +0.8207 & -0.2695 & -0.5038\end{pmatrix}$$

NORMAL EQUATION

$$\frac{x^2}{70.71^2}+\frac{y^2}{63.04^2}+\frac{z^2}{96.25^2}=1$$

TABLE 6 : CONT'D

BOREHOLE # 101-S09-MOD1

MOST PROBABLE ELLIPSOID

$$(X \;\; Y \;\; Z)\begin{pmatrix} +18.8325 & -3.7469 & -1.9457 \\ -3.7469 & +10.0133 & +5.9879 \\ -1.9457 & +5.9879 & +16.4967 \end{pmatrix}\begin{pmatrix} X \\ Y \\ Z \end{pmatrix} = 10^5$$

ROTATION MATRIX

$$\begin{pmatrix} -0.6573 & +0.4580 & +0.5985 \\ +0.7205 & +0.1938 & +0.6543 \\ -0.1837 & -0.3290 & +0.4622 \end{pmatrix}$$

NORMAL EQUATION

$$\frac{x^2}{65.63^2} + \frac{y^2}{78.82^2} + \frac{z^2}{128.78^2} = 1$$

Table 7: Summary of Uniaxial Mechanical Property Anisotropies

Borehole Number	Uniaxial Compressive Strength (kPa)	50% Tangent Modulus of Elasticity (GPa)	50% Secant Modulus of Elasticity (GPa)
206-010-MOD1	1.36	1.10	1.23
206-012-MOD1	1.48	1.62	1.49
206-013-MOD1	1.26	1.24	1.24
206-016-MOD1	2.08	1.24	1.43
001-041-MOD1	2.14	1.93	1.44
001-041-MOD2	1.30	1.28	1.48
001-072-MOD1	2.09	1.12	1.29
001-072-MOD2	1.56	1.18	1.50
001-228-MOD1	1.40	1.10	1.16
001-228-MOD2	1.30	1.14	1.18
001-275-MOD1	1.23	1.24	1.32
001-275-MOD2	1.34	1.53	1.20
101-S09-MOD1*	2.14	1.96	3.05
mean	1.54	1.31	1.33

*Due to differences in composition, results from borehole #101-S09-MOD1 were not included in the mean calculations.

Table 8: Mean, Standard Deviation and Spread of Uniaxial Mechanical Property Anisotropies

	Uniaxial Compressive Strength	50% Tangent Modulus of Elasticity	50% Secant Modulus of Elasticity
mean	1.54	1.31	1.33
standard deviation	0.35	0.25	0.13
spread	1.23 - 2.14	1.10 - 1.93	1.16 - 1.50

FIG. 2 : CUMULATIVE PROBABILITY PLOT FOR 50% TANGENT MODULUS OF ELASTICITY ANISOTROPIES

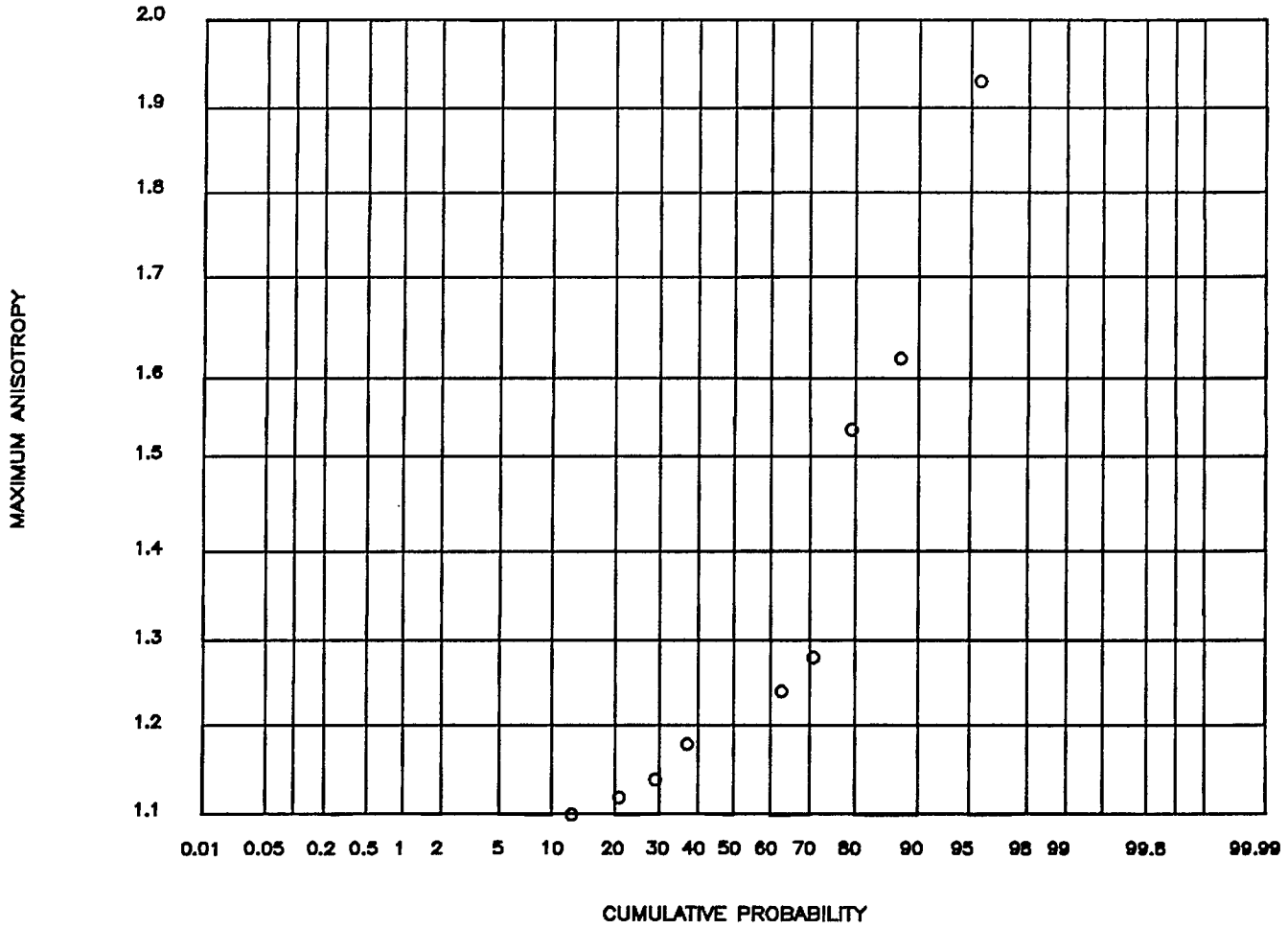

REFERENCES

1. Annor, A. and Geller, L., "Dilatational velocity, Young's modulus, Poisson's ratio, uniaxial compressive strength and Brazilian tensile strength for WN1 and WN2 samples", CANMET/MRL Technical Data 303410-M01/78, 1978.

2. Lama, R.D., Saluja, S.S., Vutikuri, V.S., "Handbook on mechanical properties of rocks", Volume I, Chapter 2, Trans Tech Publications.

3. Lang, P., "Personal communication", 1985.

4. Paul, B. and Gangal, M., "Initial and subsequent fracture curves for biaxial compression of brittle materials", Proc. 8th Symp. Rock Mech., Minneapolis, Minn., 1966.

5. Peres-Rodrigues, F., "Anisotropy of granites. Modulus of elasticity and ultimate strength ellipsoids, joint systems, slope attitudes and their correlations", Proc. 1st Cong. ISRM, Lisbon, Spain, 1966.